

Distributed SMC for Secondary Voltage and Frequency Regulation of AC Microgrid Adulterated by Communication Irregularities

Hema Mehta¹ Himani Modi² Axaykumar Mehta²

¹Rai University,
Ahmedabad - 382260, Gujarat, INDIA

²Institute of Infrastructure Technology Research and Management
Ahmedabad - 380026, Gujarat, INDIA

Abstract

The Microgrid (MG) is a small-scale power grid having multiple Distributed Generation (DG) units sharing their information through communication links. The fundamental requirement of an islanded Microgrid is the voltage, frequency synchronization and power sharing among all participating DGs. Traditionally the Microgrid operation in the islanded mode requires the primary control which regulates the voltage and frequency of each DG. However due to load variation, there is deviation in voltage and frequency of all DGs. These deviations are not compensated by primary controller alone so it is required to empanel a secondary controller which takes care of not only the disturbances but also the uncertainties. This paper presents Distributed Sliding Mode Controller (DSMC) for secondary voltage and frequency regulation of AC Microgrid adulterated by communication irregularities like time delay and packet loss. The proposed distributed SMC which is distributed in nature incorporates distributed cooperative control that ensures the coordination and synchronization of each agent (DG) in a Multi-Agent configuration. In multi-agent system configuration, the leader (one of the DG) only gets the reference information and acts as a command generator and all other agents (DGs) synchronize to leader node. Moreover, all the DGs are connected through communication network topology represented by graph theory. It is evident that the information might incur time delay as well packet loss in the communication network due to substantial distance between neighbor DGs which may deteriorate the performance of Microgrid. The proposed novel DSMC algorithm not only compensate constant and random time delay but also takes care of packet loss occur in the communication network between the DGs. The Pad Approximation technique and exponential distribution methodology are employed to overcome the effect of

deterministic and random time delay. The proposed algorithms tested in MATLAB environment on a test Microgrid having 4 DGs connected in graph topology and having distributed communication among them. The simulation results are also compared for secondary controller designed by the feedback linearization method to show the efficacy of the proposed algorithm.

Keywords: *Microgrid, Sliding mode control, Multi-agent system, Feedback linearization, Pad approximation, Exponentials distribution.*

1. Introduction

The Microgrid (MG) bridge the gap between the conventional power system and the distributed renewable generation [1], [2], [3]. The Microgrid has multi-objective task which covers different technical areas. The Microgrids control has hierarchical control strategy consists of three levels: primary, secondary, and tertiary control [4]. The primary control is mainly composed of droop control which takes care of demand and supply. And the voltage and frequency deviations due to load variations are taken care of by secondary control. In recent years, the researchers in the domain mainly focused on secondary controller to handle these deviations and proposed various schemes for the same. Lopes et al. proposed centralized approaches for secondary control of Microgrid [5].

However, it has drawbacks of complex communication network which compromise the system reliability due to single point of failure [6],[7]. Recently, distributed approaches to secondary control has also earned much attention and many methods using feedback linearization, sliding mode control etc... have been proposed in the literature.

Recently, distributed cooperative control for Multi-Agent Systems (MAS) has earned much attention due to its flexibility and robustness [10],[11]. Distributed cooperative control protocol ensure the coordination and synchronisation of each agent in MAS. In this control protocol, system agents exchange information with other agents according to communication protocol [12]. Since Microgrid resembles to a non-linear multi-agent system (MAS) in which each DG is considered as Agent of MAS. [9], distributed cooperative control method can be applied for secondary level control. Distributed cooperative control of MAS has two types of problems: (1) Regulator synchronisation problem - all agents synchronise to a common value that is not prescribed and (2) Tracking synchronisation problem - all agents synchronise to a leader that acts as a command generator [13]. Distributed cooperative control of multi-agent systems is focus on tracking synchronisation problem. Tracking synchronisation problem is also called leader following consensus. In which, only leader gets information and acts as a command generator. All other agents synchronize to a leader node and behave according to leader dynamics. In secondary control of Microgrid, only one DG gets reference value of voltage and frequency which is known as command generator. All other DGs behave according to the command generator. The DGs terminal voltages and frequencies track the reference values of voltage and frequency, respectively [14], [15].

As mentioned various control protocols have been proposed in the literature like H_1 , state feedback, PI, Sliding Mode Control (SMC) etc... for distributed control [16]. Among them SMC is considered to be one of the robust control protocol which achieves the synchronisation in finite time [18], [19], [20]. Ali Bidram [18] applied input-output feedback linearisation for secondary control of Microgrid. In which, input-output feedback linearisation can be utilized to convert the nonlinear heterogeneous dynamics of DGs to linear dynamics. Input-output feedback linearisation, the secondary control leads to a first-order tracking synchronisation problem [21]. The communication topology between DGs is designed by a graph theory [22] and the exchange of data between various DGs takes place as per communication network topology.

For designing and operate distributed secondary controller of MG, it requires different data from its

neighbor DG. Therefore, MGs need a reliable, fast and accurate data communication. However due to involvement of networked medium such as CAN, Switched Ethernet, Profibus, Profinet etc...[29], The distributed Microgrid suffers from various challenges such as time delay, packet loss, packet disorder, resource allocation and bandwidth sharing [30], [31]. Among these issues, time delay is one of the major concern that needs to be handled properly in order to avoid degradation in stability and performance of the closed loop distributed MG system. The nature of time delay generally depends on characteristics of communication medium. When the communication is carried out using lease line concept the delays are deterministic in nature. When the communication medium is shared among different components the delays are random in nature. In available literatures [32], researchers have assumed that the value of these delays are negligible so its effect is neglected. However, in real time application these delays play a major role for deterioration of system's performance. Thus, it is necessary to compensate the effect of these delays and packet loss occur in the communication medium. This motivates the authors to introduce time delay compensation technique that compensates the effect of network delay for distributed Microgrid. This paper contributes mainly following:

- Design of distributed second order twisting sliding mode control for secondary voltage and frequency restoration and comparison with the secondary controller based on feedback linearization available in literature.
- Next, modified sliding mode controller for constant and random time delays compensation that occur in the communication link between DGs. The extensive simulation results to show the efficacy and robustness of algorithm under various load conditions and time delay effects.

The structure of paper is as follows: Section-II briefs about Microgrid structure. Section III discusses the control schemes for Microgrid available in the literature. Section III presents the mathematical model used for designing the control strategy for the microgrid. Section IV discuss about the design of sliding mode controller for distributed secondary control of MG. Section V discusses the adverse effects of delay present in the communication and also the compensation method of

constant time delay and also Pade approximation. The simulation results on a test Microgrid are discussed in Section VI followed by concluding remarks along with future scope and challenges in Section VII.

2. Preliminaries of MICROGRID

Renewable energy resources have been attracting great attention due to reduction of fossil fuel resources and particularly due to the economic and environmental issues. Power can be generated from these sources in two ways: Centralized Generation and Decentralized Generation. In centralized generation, power generation is at a single location and from there it is distributed to the loads. In decentralized generation, power is generated locally to achieve local demand. It can also send power to the main grid. Major drawbacks of centralized structure are like a single point of failure, not easy to expand and consisting of a complex communication network. These drawbacks are compensated in a decentralized generation [1], [2].

Due to growth in the number of renewable energy sources, distributed generators (DGs) and increase customer load, Microgrids (MGs) have recently got significant attention. The Microgrid is a combination of different DGs, customer load demand and Energy storage system [3]. Fig. 1 shows the block diagram of Microgrid. It is also called main building block of smartgrid. The purposes supporting the arrangement of the MGs are (1) reducing transmission and distribution losses; (2) preventing electrical network congestion by shifting the generation nearer to the consumer loads; (3) improves the reliability of the system; (4) gradually reducing the chance of blackouts [21].

Microgrids can operate in both grid connected mode and Is-landed operating mode. In Grid connected mode MG supplies or draws power to the main grid depending on generation and load demand. In Fig. 1, If Point of Common Coupling (PCC) is closed then Microgrid is in grid connected mode. When emergency and power shortage occurs the MG is disconnected from the main grid known as islanded mode. In Fig. 1, PCC is open means Microgrid operates separately [4].

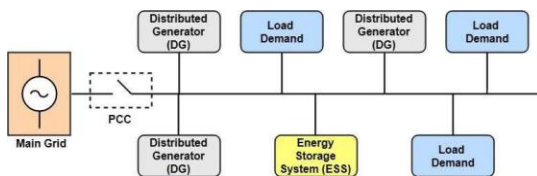


Fig. 1: Operating mode of Microgrid

There are different advantages offered by Microgrid to a public utility such as: Improved energy efficiency, improved reliability, minimized overall energy consumption, reduced greenhouse gases. Microgrid can be classified in two categories:

2) AC Microgrid: Most of RESs produces DC power which are not compatible with AC systems, thus power electronics devices become the important element for MGs [8]. Examples of the DGs which can produce the AC power like wind, bio-gas, hydro and wave turbines. These DGs require AC-DC-AC power converters to enable their stable coupling with distribution networks. DC loads use AC- DC power converters to connect with the AC networks, while AC loads directly connect with AC network. In power electronics based MGs which whole AC power inserted through the inverters, so control operations of Microgrid are to be done by the control of inverters [9].

The control objectives of AC MGs are:

- (i) Stabilize the voltages and synchronize inverters frequencies to a rated value.
- (ii) Load sharing among the inverters proportionally to their ratings.

3) DC Microgrid: DG's directly feed power to DC bus using suitable power electronics converter and the common bus operates on DC voltage as shown in Fig. 3 [15].

3. Review on Control Schemes of Microgrid

This section presents the different control scheme for MG and also preliminaries of graph theory to represent multi-agent system.

A. Control Schemes of Microgrid

The development and increasing utilization of power electronic devices, the voltage and current regulation, power flow control and other advanced control functions can be achieved in Microgrid. Microgrid control and management is actually multi-objective task which covers different technical areas, time scales and physical levels. Multi-level scheme is proposed for Microgrid [15]. The selection of the control structure can be various according to the MG type (residential, military or commercial) and physical features (location, size, topology). There are basic four types of control structures:

1. Centralized control structure: These control structure requires data from all units of Microgrid.

The block diagram of centralized control structure shown in Fig. 4. Based on the collected information, control and management procedures can be executed in the controller to achieve appropriate and efficient operation. The advantages of centralized control are good observability and controllability of the entire system. However, there are major drawbacks of centralized structure are single point of failure, reduced flexibility, less expendability and the central controller failure will cause the loss of entire system stability. Hence, for localized and small size Microgrid, centralized control is used because information is limited. Small size Microgrid have low communication and computation cost [47], [48].

2. Decentralized control structure: These control structure does not require information from other units as shown in Fig. 5. The controller's control action only depends upon local information. The advantage of these scheme is it does not require real-time communication. Droop control is example of decentralized control methods. Droop control achieves power sharing between DGs without communication. Accuracy is lesser compared to other structures [15].
3. Distributed control structure: The controller talks with each other using communication link. Each unit gets information of its neighbor's information so communication becomes simple. The required information is shared among all units. These control structure serve a coordinated behavior of all the units. In communication topology like WiFi, Zig-ee, etc...[49] and information exchange algorithms like P2P, gossip, consensus etc... are used. Main challenge of distributed control structure is the coordination among units. Consensus algorithms are widely applied for distributed control of MG
4. Hierarchical control structure: The modern energy systems require higher intelligence and systems are becoming more complex. When the system involves a complicated decision making process, all functions cannot be achieved in a distributed or decentralized manner. Fig. 7 shows widely used hierarchical control structure of Microgrid. Fig 8 shows the hierarchical control structure of Microgrid. Hierarchical control strategy consists of

three levels, namely primary, secondary and tertiary control [2].

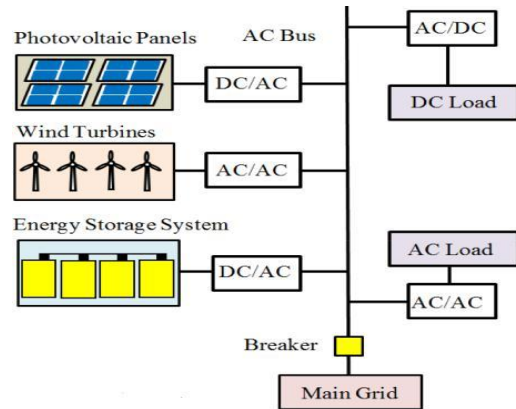


Fig. 2: AC Microgrid

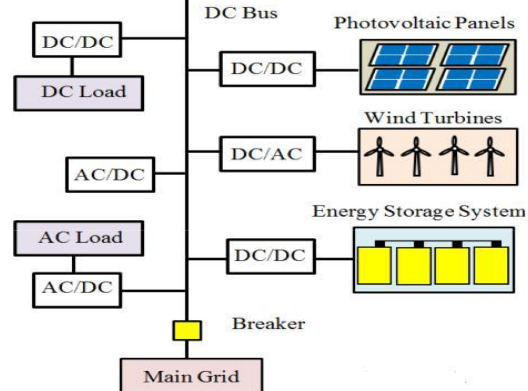


Fig. 3: DC Microgrid

The first level of the structure is primary control level which maintains voltage and frequency stability of the Microgrid subsequent to the islanding process [3],[21]. Each DG has its own primary controller. It works on locally measured signals. This control level is made of internal control loops and droop control [9]. The next control level of hierarchy is known as secondary control level. The main function of secondary control is to compensate deviation caused by model uncertainty and load variation and compensate the voltage and frequency deviations caused by the operation of the primary controls. Secondary control restores the voltage and frequency levels to their nominal values by determining the set points for primary control. Tertiary control manages power flow control between main electricity grid and Microgrid.

4. Preliminary of Graph Theory

The communication network of a multi-agent cooperative system can be modeled by a directed graph (digraph). A digraph is usually expressed as $G_r = (V_G; E_G; A_G)$ with a nonempty finite set of N nodes $V_G = v_1; v_2; \dots; v_N$, a set of edges or arcs $E_G \subset V_G \times V_G$, and the associated adjacency matrix $A_G = [a_{ij}] \in R^{N \times N}$. In Microgrid, DGs are considered as the nodes of the communication digraph. The edges of the corresponding digraph of the communication network denote the communication links.

In this paper the digraph is assumed to be time invariant i.e. $A+G$ is constant. An edge from node j to node i is denoted by $(v_j; v_i)$ which means that node i receives the information from node j , a_{ij} is the weight of edge $(v_j; v_i)$ and $a_{ij} \leq 0$ if $(v_j; v_i) \in E_G$ otherwise $a_{ij} = 0$. Node i is called a neighbor of node j if $(v_i; v_j) \in E_G$. The set of neighbors of node j is denoted as $N_j = \{(v_i; v_j) \in E_G\}$. For a digraph, if node i is a neighbor of node j then node j can get information from node i but not necessarily vice versa. A digraph is said to have a spanning tree if there is a root node with a direct path from that node to every other node in the graph [11], [22]. The Laplacian matrix L is a square $n \times n$ matrix that may be defined, using the notion of degree matrix D and adjacency matrix A , as under:

$$L = D - A \tag{1}$$

Note that the row sums of L are all zero. The Laplacian matrix has row sums equal to zero so that all graphs have the first eigenvalue at 0. All undirected graphs have a symmetric Laplacian matrix L and so their graph eigenvalues are real [11], [22].

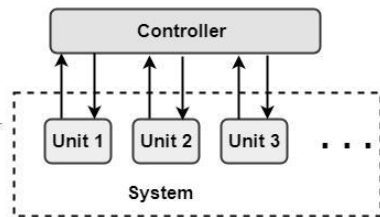


Fig. 4: Centralized control

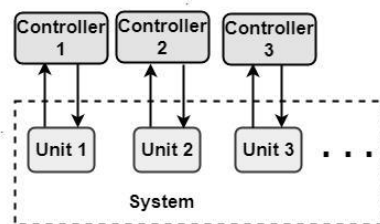


Fig. 5: Decentralized control structure

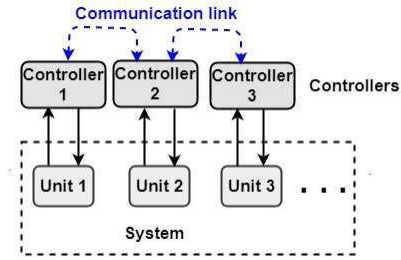


Fig. 6: Distributed control structure

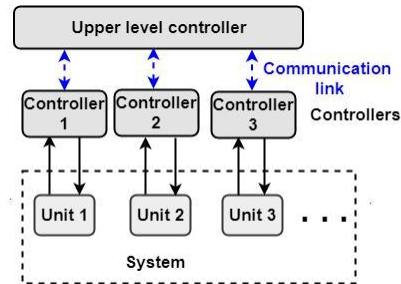


Fig. 7: Hierarchical control structure

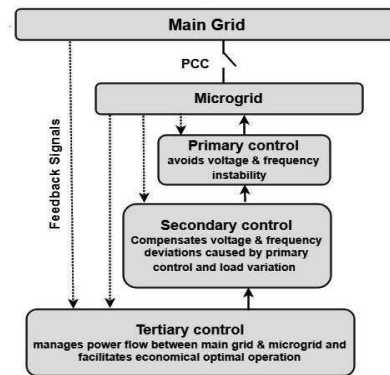


Fig. 8: Hierarchical control levels of a Microgrid. [2]

5. Mathematical Model of Microgrid

A. Dynamical model of an inverter-based distributed generator:

In this paper, the mathematical model of a Microgrid proposed in [2] is used for the formulation of algorithms. A Microgrid is a combination of DGs and loads. Each DG system includes a renewable energy source (RES), an energy storage system (ESS), and a power electronic interface, which normally consist of a dc-ac inverter. Figure 9 shows block diagram of inverter based DG. As stated in [1], DC-bus dynamics can be securely ignored. Assuming DG side has an ideal source. It should be seen that the nonlinear components of each DG are arranged in its own specific $d-q$ (direct-quadrature) reference frame. It is assumed that the reference frame of the i^{th} DG is rotating at the ω_i

frequency. One DG's reference frame is taken as common reference. The frequency of common reference frame is taken as ω_{com} . By concerning the common reference frame, The point of the i^{th} DG reference outline, concerning the regular reference outline, The angle of the i^{th} DG reference frame is,

$$\delta_i = \omega_i - \omega_{com} \quad (2)$$

Power processing section consist of a VSI, an output LC filter and coupling inductor as output connector (Lc).

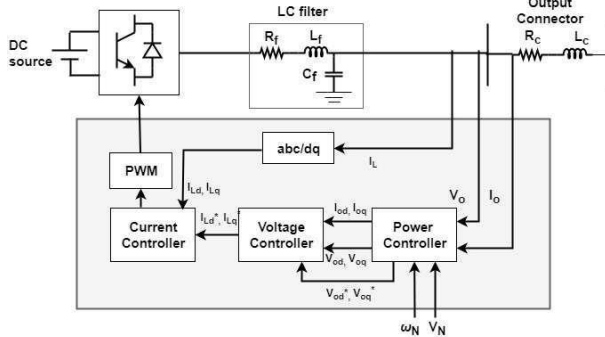


Fig. 9: Block diagram of inverter based DG [1]

Assume that DG side has ideal source and also DC side dynamics are neglected. The dynamical model is described in [1]. Primary control level consists of three controllers: power, voltage and current controller. Power control will share the fundamental real and reactive power with other DGs. Voltage and current controllers are designed to reject high frequency disturbances. Power controller is shown in Fig. 10. It provides the operating frequency ω_i for the inverter bridge and the voltage references V_{odi}^* and V_{oqi}^* for the voltage controller. Two low-pass filters with the cut-off frequency of ω_{ci} are utilized to remove the fundamental component of the output active and reactive powers, indicated as P_i and Q_i , respectively. Power control is based on droop control technique. Droop technique gives the relation between the frequency and active power P_i and also between the voltage amplitude and reactive power Q_i . The frequency and voltage droop characteristics for the i^{th} DG are written as,

$$\omega_i = \omega_{Ni} - m_{pi} P_i \quad (3)$$

$$V_{odi}^* = V_{Ni} - n_{Qi} Q_i \quad (4)$$

$$V_{odi}^* = 0 \quad (5)$$

Where, ω_i are angular frequency of the DG dictated by the primary control, P_i and Q_i are active and reactive power measured at each DG's terminal. m_{pi} and m_{Qi} are Droop coefficients of i^{th} DG and are selected based on the active and reactive power ratings of each DG. V_{Ni} and ω_{Ni} are primary control references for voltage and frequency.

The power controller block provides the voltage references V_{odi}^* and V_{oqi}^* for the voltage controller and also the operating frequency ω_i for the inverter bridge.

The low-pass filters are used to extract the fundamental component of the output active (P_i) and reactive power (Q_i). The differential equations of the power controller can be written as,

$$\dot{P} = -\omega_{ci} P_i + \omega_{ci} (V_{odi} I_{odi} + V_{oqi} I_{oqi}) \quad (6)$$

$$\dot{Q} = -\omega_{ci} Q_i + \omega_{ci} (V_{oqi} I_{odi} - V_{odi} I_{oqi}) \quad (7)$$

Where, V_{odi} , V_{oqi} , I_{odi} , and I_{oqi} are the direct and quadrature axis components of V_{oi} and I_{odi} shown in Fig. 11. PI controller is used for voltage and frequency control of Microgrid [34]. The differential algebraic equations of the voltage controller are represented as,

$$\dot{\psi}_{di} = V_{odi}^* - V_{odi} \quad (8)$$

$$\dot{\psi}_{qi} = V_{oqi}^* - V_{oqi} \quad (9)$$

$$I_{Ldi}^* = F_i I_{odi} - \omega_b C_{fi} V_{oqi} + K_{PVi} (V_{odi}^* - V_{odi}) + K_{IVi} \psi_{di} \quad (10)$$

$$I_{Lqi}^* = F_i I_{oqi} + \omega_b C_{fi} V_{odi} + K_{PVi} (V_{oqi}^* - V_{oqi}) + K_{IVi} \psi_{qi} \quad (11)$$

Where, ψ_{di} and ψ_{qi} are the auxiliary state variables defined for PI controllers. The current controller is governed by [34].

$$\dot{\gamma}_{di} = i_{ldi}^* - i_{ldi} \quad (12)$$

$$\dot{\gamma}_{qi} = i_{lqi}^* - i_{lqi} \quad (13)$$

$$v_{idi}^* = -\omega_b L_{fi} i_{lqi} + K_{PCi} (i_{ldi}^* - i_{ldi}) + K_{ICi} \gamma_{di} \quad (14)$$

$$v_{iqi}^* = -\omega_b L_{fi} i_{ldi} + K_{PCi} (i_{lqi}^* - i_{lqi}) + K_{ICi} \gamma_{qi} \quad (15)$$

where γ_{di} and γ_{qi} are the auxiliary state variables defined for the PI controllers and i_{ldi} and i_{lqi} are the direct and quadrature components of i_{li} in Figure 11. The differential equations for the output LC filter and output connector are as follows:

$$\dot{I}_{Ldi} = -\frac{R_{fi}}{L_{fi}} I_{Ldi} + \omega_i I_{Lqi} + \frac{1}{L_{fi}} V_{idi} - \frac{1}{L_{fi}} V_{odi} \quad (16)$$

$$\dot{I}_{Lqi} = -\frac{R_{fi}}{L_{fi}} I_{Lqi} - \omega_i I_{Ldi} + \frac{1}{L_{fi}} V_{iqi} - \frac{1}{L_{fi}} V_{oqi} \quad (17)$$

$$\dot{V}_{odi} = \omega_i V_{oqi} + \frac{1}{C_{fi}} V_{Ldi} - \frac{1}{C_{fi}} I_{odi} \quad (18)$$

$$\dot{V}_{oqi} = -\omega_i V_{odi} + \frac{1}{C_{fi}} I_{Lqi} - \frac{1}{C_{fi}} I_{oqi} \quad (19)$$

$$\dot{I}_{odi} = -\frac{R_{ci}}{L_{ci}} I_{odi} + \omega_i I_{oqi} + \frac{1}{L_{ci}} V_{odi} - \frac{1}{L_{ci}} V_{bdi} \quad (20)$$

$$\dot{I}_{oqi} = -\frac{R_{ci}}{L_{ci}} I_{oqi} + \omega_i I_{odi} + \frac{1}{L_{ci}} V_{oqi} - \frac{1}{L_{ci}} V_{bqi} \quad (21)$$

Eqn. (3) - (21) form the large-signal dynamical model of the i^{th} DG. The large-signal dynamical model can be written in a compact form as [4],

$$\begin{aligned} \dot{x}_i &= f_i(x_i) + k_i(x_i) D_i + g_i(x_i) \\ y_i &= h_i(x_i) \end{aligned} \quad (22)$$

Where the state vector is

$$x_i = [\delta_i \ P_i \ Q_i \ \psi_{di} \ \psi_{qi} \ \gamma_{di} \ \gamma_{qi} \ I_{Ldi} \ I_{Lqi} \ V_{odi} \ V_{oqi} \ I_{odi} \ I_{oqi}]^T \quad (23)$$

The term $D_i = [\omega_{com} \ V_{bdi} \ V_{bqi}]^T$ is considered as a known disturbance. The detailed expressions for $f_i(x_i)$, $g_i(x_i)$ and $K_i(x_i)$ can be extracted from Eqn. (6) to (21).

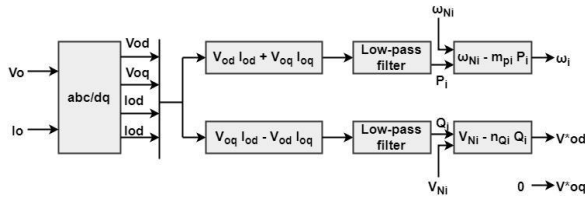


Fig. 10: Power controller

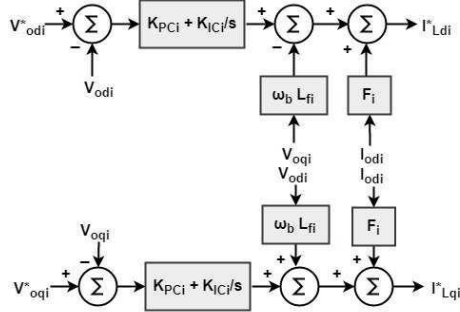


Fig. 11: Voltage controller

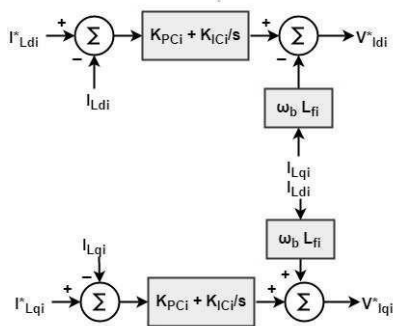


Fig. 12: Current controller

B. Simulation of test Microgrid

The Microgrid shown in Fig. (13) is used to verify the effectiveness of the selected model for further experiments. The specifications of the DGs, lines and loads are summarized in Table I. Here, DC input voltage of DG is 850 V. Fig. (14), - (19) show voltage, angular frequency, current, active power and reactive power of each DG. Reference values of voltage and frequency for Microgrid is $V_{Ni} = 220V_{RMS} \sim 380V_{ph-ph}$ and $\omega_{Ni} = 2 \times \pi \times 50$ Hz. At $t = 1.5$ sec the load variation of 20 KW occurs at DG 2. The results show that only primary controller not able to reach predefined reference value of voltage and angular frequency due to model uncertainty, transmission losses and load variation. It is necessary to design robust secondary controller for restoration of voltage and frequency.

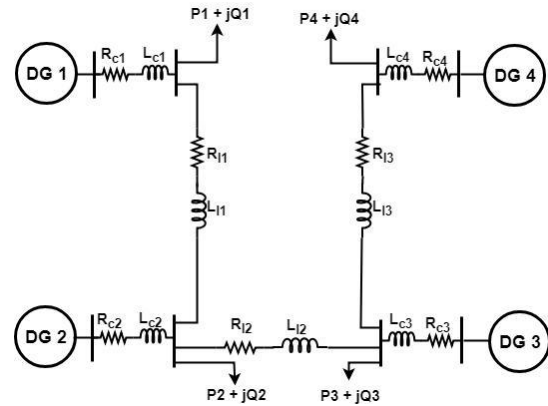


Fig. 13: Islanded Microgrid

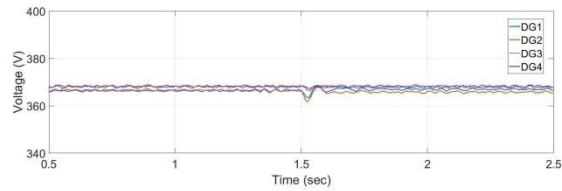


Fig. 14: Voltage waveform of primary controller

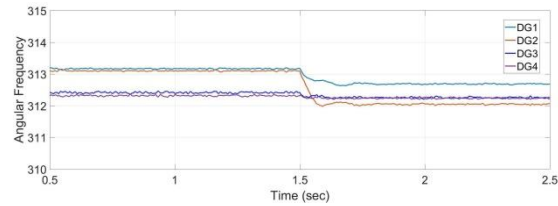


Fig. 15: Angular frequency waveform of primary controller

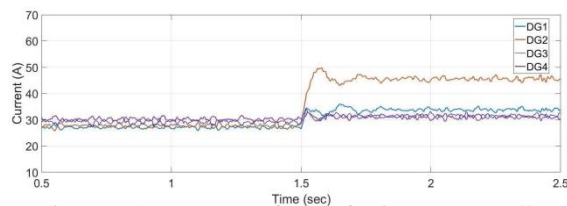


Fig. 16: Current waveform of primary controller

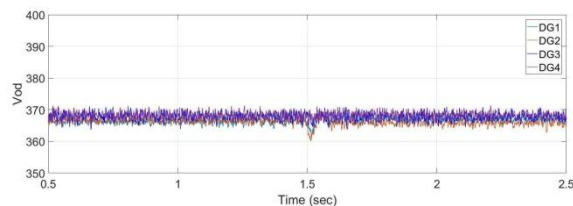


Fig. 17: Direct axis voltage waveform of primary controller

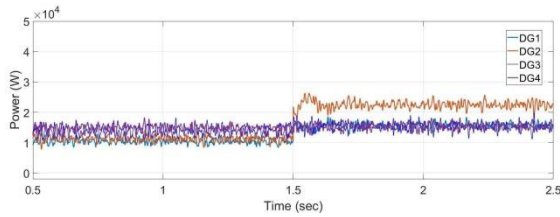


Fig. 18: Active power waveform of primary controller

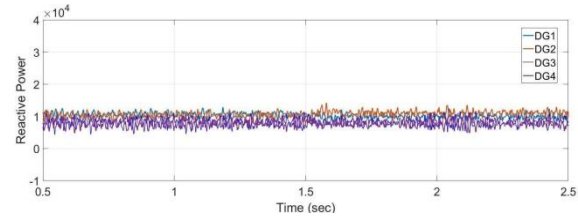


Fig. 19: Reactive power waveform of primary controller of Microgrid

TABLE I: Specifications of the Microgrid test system

	DG 1 & 2 (45 KVA rating)		DG 3 & 4 (34 KVA rating)	
Droop control	m_P 9.4×10^{-5}	n_Q 1.3×10^{-3}	m_P 12.50×10^{-5}	n_Q 1.5×10^{-3}
Voltage control	K_{pv} 0.2	K_{pc} 5	K_{pv} 0.5	K_{pc} 3
Current control	K_{iv} 42	K_{ic} 2000	K_{iv} 39	K_{ic} 1600
Connector	R_c 0.03Ω	L_c 0.35mH	R_c 0.03Ω	L_c 0.35mH
Loads	P 12KW	Q 12KVAR	P 15.3KW	Q 7.6KVAR
LC filter	R_f 0.1Ω	L_f 2.2mH	R_f 0.1Ω	L_f 2.2mH
Line Losses	Line 1		Line 2	
	R_{l1} 0.23Ω	L_{l1} 0.318mH	R_{l2} 0.35Ω	L_{l2} 1.847mH
			R_{l3} 0.23Ω	L_{l3} 0.318mH

6. Secondary Voltage and Frequency Control using Distributed SMC

A Microgrid resembles a nonlinear and heterogeneous Multi-Agent System (MAS), where each DG is considered as an agent. For tracking synchronization problem, a secondary control is designed where all DGs attempt to synchronize their terminal voltage amplitude and frequency to a pre-specified reference value. For this reason, each DG required to communicate with its neighbors only. The required communication network topology can be demonstrated by a communication graph theory. A. Distributed SMC for voltage restoration.

It is known fact that voltage and frequency deviates at the instant of load variation which may not be compensated by only primary controller. Primary controller is also not able to achieve reference value and synchronize with connected DGs. For compensate the deviation and achieve reference value, it is required to design a secondary controller which takes care of not only the disturbance but also the model uncertainties. The sliding mode control is one of the robust control techniques which takes care of all such uncertainties.

In this section, distributed secondary control is designed to synchronize the voltage magnitudes of all DGs to its reference value V_{ref} and also communicate using the information of neighbor DGs. The

synchronization of voltage magnitudes of DGs are equivalent to synchronizing the direct term of output voltage V_{odi} . The secondary voltage control is to choose proper control input V_{ni} for the power controller of the primary controller. For synchronization tracking of voltage of all DG is necessary thing. Primary controller is not sufficient to reduce this tracking error. Reduction of tracking error becomes objective of secondary controller. Let us define neighborhood global voltage tracking error,

$$e_{vi} = \sum_{j \in N_i} a_{ij}(V_{odi} - V_{odj}) + g_i(V_{odi} - V_{ref}) \quad (24)$$

here, a_{ij} is an element of adjacent matrix. Adjacency matrix A will reflect the communication network topology of all DGs. g_i is the pinning gain. For leader DG which get reference value of $g_i > 0$ [3].

1) SMC design: Classic sliding modes provide robust and high-accuracy solutions for a wide range of control problems under uncertainty conditions. however, the main drawback at high-frequency control switching may easily cause unacceptable chattering effect, the problem may be overcome by higher order SMC controller. Consider now a simple 2^{nd} order sliding controller, namely the “twisting” controller [22], [17]. Sliding mode controller is designed to synchronise the voltage magnitude of DGs to reference value V_{ref} . According the model uncertainty and load variation secondary controller give command to the droop control of primary controller. Therefore Eqn. (4) and (5) can be written as,

$$V_{odi} = V_{Ni} - n_{Qi}Q_i \quad (25)$$

$$V_{odi} = 0 \quad (26)$$

To achieve the synchronisation for V_{odi} , it is assumed that DGs can communicate with each other through a prescribed communication digraph G . The control law is chosen based on the own information of each DG and the information of its neighbors in the graph.

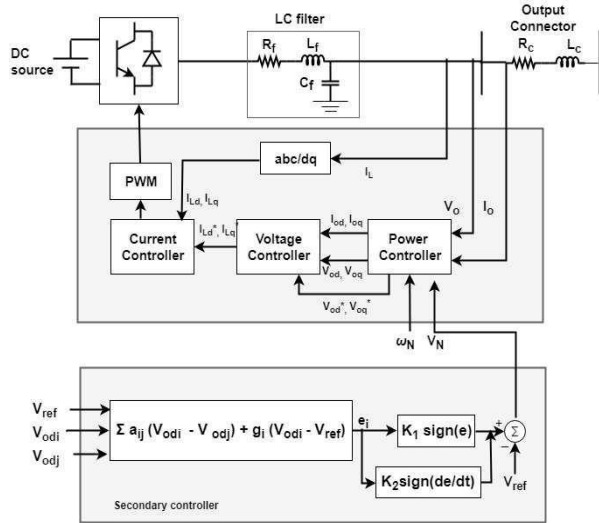


Fig. 20: Secondary voltage control using SMC

Using global tracking error (24), the control law is defined as [17],

$$V_{ni} = K_1 \text{sign}(e_{vi}) + K_2 \text{sign}(\dot{e}_{vi}). \quad (27)$$

The control signal is sent to the power control of primary controller as shown in Fig. (20). The twisting algorithm of sliding mode control compensate the deviation caused by primary controller and load variation.

Stability Analysis: The following lemmas and theorem considered to prove that the proposed controller in (27) can provide synchronisation for V_{odi} . Microgrid is a multi-agent system so global tracking error is defined in vector form.

Eqn. (27) also written as,

$$e = (\mathcal{L} + G)(V_{od} - 1_N \otimes V_{ref}) \quad (28)$$

Where, $V_{od} = [V_{od1} \ V_{od2} \ V_{od3} \ \dots \ V_{odN}]$, $e = [e_{v1} \ e_{v2} \ e_{v3} \ \dots \ e_{vN}]$ and $V_{ref} = 1_N \otimes V_{ref}$. 1_N is the vector of ones with the length of N . The Kronecker product is \otimes . The global disagreement vector is δ .

Lemma 1 [3]: Let the digraph G have a spinning tree and $g_i \neq 0$ for at least one DG.

$$\|\delta\| = \|e\| / \sigma_{\min}(\mathcal{L} + G) \quad (29)$$

Where, $\sigma_{\min}(\mathcal{L} + G)$ is the minimum singular value of $(\mathcal{L} + G)$ and $e = 0$ if and only if all nodes synchronise.

Theorem 1: Let the digraph G have a spanning tree and $g_i \neq 0$ for at least one DG. Let the control law V_{Ni} be chosen as in (27). Then, the global neighborhood tracking error e in (24) is asymptotically stable. Moreover, the DG output voltage direct terms V_{odi} synchronise to V_{ref} in finite time.

Proof: Sliding surface for Microgrid,

$$S = \int e = \int [(\mathcal{L} + G)(V_{od} - 1_N \otimes V_{ref})] \quad (30)$$

Differentiating sliding surface, we get

$$\dot{S} = (\mathcal{L} + G)(V_{od} - 1_N \otimes V_{ref}) \quad (31)$$

Substituting the value of V_{od} ,

$$\dot{S} = (\mathcal{L} + G)(V_N - n_Q Q - 1_N \otimes V_{ref}) \quad (32)$$

Now substituting control law from eqn. (27),

$$\dot{S} = (\mathcal{L} + G)(-K_1 \text{sign}(e) - K_2 \text{sign}(\dot{e}) - n_Q Q - 1_N \otimes V_{ref}) \quad (33)$$

From above equation (33), we can say that If K_1, K_2 and n_Q are positive definite then \dot{S} becomes negative definite. So the Lyapunov function V is negative definite. This prove that the global neighborhood error e is asymptotically stable.

From Lemma 1, the global disagreement vector is asymptotically stable and the DG output voltage direct terms V_{odi} synchronise to V_{ref} .

This completes the proof.

2) **Feedback linearization:** Feedback linearization technique is designed here to verify the results of the secondary sliding mode control. It is also designed to synchronize the voltage amplitudes of DGs V_{odi} to the reference voltage V_{ref} . Brief derivation of feedback linearisation method given in [3].

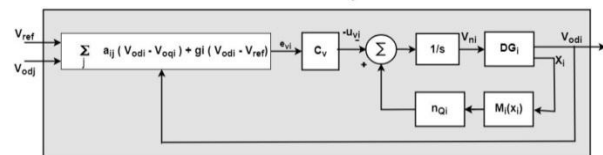


Fig. 21: Block diagram of feedback linearization for secondary voltage control

The nonlinear dynamics of the i^{th} DG, given in Eqn. (22) are considered here. It should be noted that the dynamics of the voltage and current controller are much faster than the dynamics of the power controller [1]. Therefore, by neglecting the fast dynamics of the

voltage and current controller, Eqn. (22) can be written as

$$V_{odi} = V_{ni} - n_{Qi}Q_i \quad (34)$$

$$V_{odi} = 0 \quad (35)$$

Differentiating the upper equation in Eqn. (34) yields

$$\dot{V}_{odi} = \dot{V}_{ni} - n_{Qi}\dot{Q}_i \equiv u_{vi} \quad (35)$$

The auxiliary controls u_{vi} are chosen based on own information of each DG and the information of its neighbors in the graph as

$$u_{vi} = c_v e_{vi} \quad (36)$$

The block diagram of the secondary voltage control based on the distributed cooperative control is shown in Fig. 23 [1]. The control input V_{ni} is written as

$$V_{ni} = \int (u_{vi} + n_{Qi}\dot{Q}_i) dt \quad (36)$$

Where,

$$\dot{Q}_i = -\omega_c Q_i + \omega_c (v_{oqi}i_{odi} - v_{odi}i_{oqi}) = M_i(X_i) \quad (37)$$

B. Distributed secondary frequency control design

In this section, a distributed sliding mode control is designed to synchronise the frequency of DGs ω_i to the reference frequency V_{ref} . The secondary frequency control is to choose appropriate control inputs ω_{Ni} based on the following procedure.

Let us define global neighborhood tracking error,

$$e_{\omega i} = \sum_{j \in N_i} a_{ij}(\omega_i - \omega_j) + g_i(\omega_i - \omega_{ref}) \quad (38)$$

Where, a_{ij} is an element of adjacent matrix. Adjacency matrix A will reflect the communication network topology of all DGs. g_i is the pinning gain. The leader DG gets reference value of $g_i > 0$ [22]. For tracking synchronization problem, it is required to design suitable a controller which can mitigate this error.

1) Sliding mode control: The nonlinear dynamics of the i^{th} DG in (22), are considered. Rewrite the frequency droop characteristic equation given in (3),

$$\omega_i = \omega_{Ni} - m_{pi}P_i \quad (39)$$

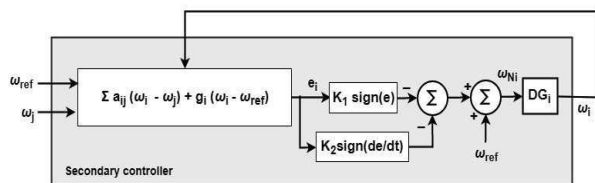


Fig. 22: Block diagram of the distributed SMC for secondary frequency control

To achieve the synchronisation for ω_i , it is assumed that DGs can communicate with each other through a prescribed communication digraph G . The control law is chosen based on the own information of each DG and the information of its neighbors in the graph. Using global tracking error (28), the control law [17] is defined as,

$$\omega_{Ni} = K_1 \text{sign}(e_{\omega i}) + K_2 \text{sign}(\dot{e}_{\omega i}). \quad (40)$$

It should be noted that once the secondary frequency control is applied, the DG output powers are expected to be allocated according to the same pattern used for primary control [50]. After applying the primary control, the DG output powers satisfy the following equality

$$m_{p1}P_1 = m_{p2}P_2 = \dots = m_{pN}P_N \quad (41)$$

Since the active power droop coefficients m_{pi} are chosen based on the active power rating of DGs, $P_{max,i}$ (41) is equivalent to

$$\frac{P_1}{P_{max1}} = \frac{P_2}{P_{max2}} = \dots = \frac{P_N}{P_{maxN}} \quad (42)$$

This ω_{Ni} is reference value for the primary controller. It is injected at power control loop of primary controller. Results shows the robustness of SMC based secondary frequency restoration.

2) Feedback linearization: The dynamics of DGs in Microgrid are nonlinear and nonidentical which is given in Eqn. (22). Input-output feedback linearization is used to transform the nonlinear heterogeneous dynamics of DGs to linear dynamics.

By differentiating frequency droop characteristic which is given in Eqn. (3).

$$\dot{\omega}_i = \dot{\omega}_{Ni} - m_{pi} \dot{P}_i = u_{\omega i} \quad (43)$$

Where $u_{\omega i}$ is denoted as auxiliary control. The value of $u_{\omega i}$ is chosen based on each DGs own information and the information of neighbor according to communication graph theory as,

$$u_{\omega i} = -C_{\omega} e_{\omega i} \quad (44)$$

Where $C_{\omega} \in R$ and the global neighborhood tracking error is denoted by,

$$e_{\omega i} = \sum_{j \in N_i} a_{ij}(\omega_i - \omega_j) + g_i(\omega_i - \omega_{ref}) \quad (45)$$

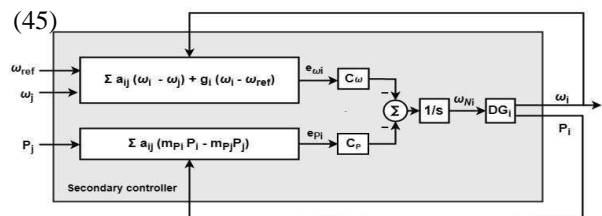


Fig. 23: Block diagram of feedback linearization for secondary frequency control

Theorem 2: Let the digraph G have a spanning tree and $g_i \neq 0$ for at least one DG. Let the auxiliary control u_{ω_i} be chosen as (44). Then, the global neighborhood tracking error (e_{ω_i}) in (44) is asymptotically stable.

Proof: The proof of Theorem 2 is given in [2].

According to (44) and (45), ω_{Ni} is written as,

$$\omega_{Ni} = \int (u_{\omega_i} + m_{P_i} \dot{P}_i) dt \quad (46)$$

It should be noted that once the dynamics of frequency control changed so DG powers are deviated from its original values. To avoid this problem, design an additional distributed control for $m_{P_i} \dot{P}_i$ in Eqn. (46). Now, the auxiliary control for power and local neighborhood tracking error are defined as,

$$u_{P_i} = -c_p e_{P_i} \quad (47)$$

$$e_{P_i} = \sum_{j \in N_i} a_{ij} (m_{P_i} P_i - m_{P_j} P_j) \quad (48)$$

As shown in Fig. 25, The control input ω_{Ni} is written as

$$\omega_{Ni} = \int (u_{\omega_i} + u_{P_i}) dt \quad (49)$$

The control gains C_ω and C_P are tuned for the convergence speed of DG frequencies and filtered output power.

3. Simulation results:

The Microgrid shown in Fig. (13) is used to verify the effectiveness of the proposed secondary control. The specifications of the DGs, lines and loads are surmised in Table I. The value of sliding gain of SMC technique and control gains of feedback linearization method

TABLE II: Parameter of the two controller

Controller	DG 1		DG 2		DG 3		DG 4	
Sliding Mode	K_1	1.05	K_1	1.1	K_1	1.5	K_1	1.4
	K_2	0.001	K_2	0.001	K_2	0.001	K_2	0.001
Feedback Linearization	$c_{\omega 1}$	100	$c_{\omega 1}$	100	$c_{\omega 3}$	90	$c_{\omega 4}$	90
	$c_{P 1}$	7	$c_{P 2}$	7	$c_{P 3}$	5	$c_{P 4}$	5

given in Table II. Here, DC input voltage of DG is 850 V. Each DG communicate with its neighbors only and the communication network topology represented by dotted line in Fig. (26). It is assumed that the DGs communicate with each other through the communication graph theory. Adjacency matrix corresponding to the graph shown in Fig. (26) and degree matrices are represented as:

$$A = \begin{bmatrix} 0 & 1 & 0 & 0 \\ 1 & 0 & 1 & 0 \\ 0 & 1 & 0 & 1 \\ 0 & 0 & 1 & 0 \end{bmatrix}; \quad D = \begin{bmatrix} 1 & 0 & 0 & 0 \\ 0 & 2 & 0 & 0 \\ 0 & 0 & 2 & 0 \\ 0 & 0 & 0 & 1 \end{bmatrix}$$

The Laplacian matrix is

$$\mathcal{L} = D - A = \begin{bmatrix} 1 & -1 & 0 & 0 \\ -1 & 2 & -1 & 0 \\ 0 & -1 & 2 & -1 \\ 0 & 0 & -1 & 1 \end{bmatrix}$$

The row sums of Laplacian matrix L are all zero. DG1 gets the reference value so it is known as leader node. pinning gain of DG1 is $g_1 = 1$ and for other DGs pinning gain is $g_2 = g_3 = g_4 = 0$.

Simulation results are carried out in three stages:

Stage 1: At the starting ($t=0s$ to $t=1s$), Only primary controller is active with primary control set points $V_{Ni} = 220 V_{RMS} \sim 380V_{ph-ph}$ and $\omega_{Ni} = 2 \times \pi \times 50$ Hz.

Stage 2: At $t = 1$ s the voltage and frequency restoration secondary controller is activated with $V_{ref} = 220 V_{RMS}$ 380Vph-ph and $\omega_{Ni} = 2 \times \pi \times 50$ Hz.

Stage 3: At $t = 1.5s$ the load variation of 20 KW occurs at DG 2.

In this section, we discuss the obtained results depicted from Fig. (24) - (25). The simulation results show the comparison between the sliding mode control method and feedback linearization method. Fig (24), and (28), show the result of (A) sliding mode control and (B) shows the result of feedback linearization control. From this results, it can be observed that SMC sets reference value in a very short time means its settling time is negligible so it is called finite time controller, but Feedback linearization technique takes more time to settle. At stage 3, SMC almost kills the effect of load variation but in feedback linearization technique MG system affected by the load variation. Fig. 25 shows the effect of these three stages on MG system. Voltage restoration technique using SMC and feedback linearization technique described in subsection 4.2.1 and 4.2.2 respectively. In SMC technique, the effect of load variation compensated but due to load variation in feedback linearization technique, the voltage is deviated from its reference value.

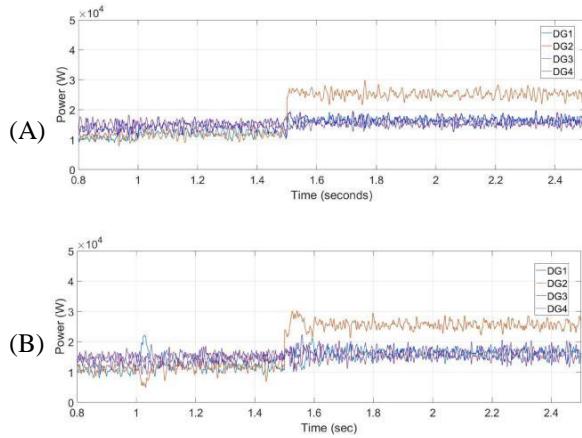


Fig. 24: Power waveform using (A) Sliding mode control (B) Feedback linearization.

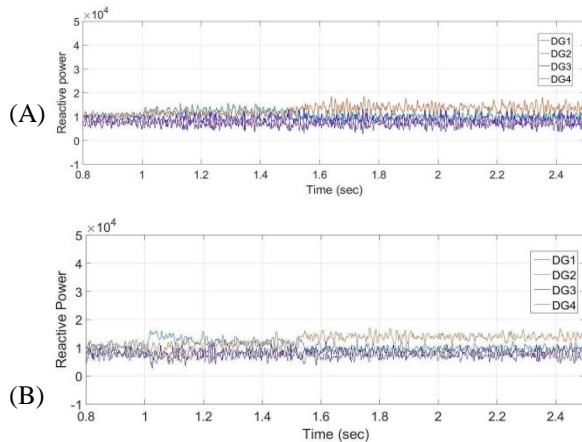


Fig. 25: Reactive power waveform using (A) Sliding mode control (B) Feedback linearization.

7. Effect of Communication Network Delay and Method of Compensation

Communication channels are used to support the information exchange between a DGs of Microgrid. Distributed secondary controller is proposed for Microgrid. Where each DG gets information from its neighbors. communication topology is designed by graph theory. normally communication channels are divided in two parts: (1) Wired communication and (2) There are several wired technologies used in power systems like serial communication RS-232/422/485, power-line communication (e.g. PLC, BPLC), bus technology (e.g. CANBus, Mod-Bus, ProfiBus) and Ethernet (e.g. LAN, optical cable) [45]. The popular wire-less technologies used in power systems are Wi-fi, WiMax, ZigBee, Z-Wave, Bluetooth, Insteon, radio frequency and microwave [46]. In Microgrid communication, we talk about the wired

communication between DGs. In communication system, time delay is congenital issue of the communication infrastructures. There are mainly two types of time delay: (1) Constant delay and (2) Random delay. Time delay compensation is necessary for any stable system. This chapter mainly focus on constant delay effect on Microgrid and proposed method for compensation of time delay. The efficacy of proposed algorithm is shown by simulation results.

A. Effect of time delay

The communication between neighboring DGs are in distributed control strategy. However, the distance between neighboring DGs produce adverse effect like time delay. Time delay effect is unavoidable for secondary control level. Fig. (26) shows the time delay in distributed secondary control.

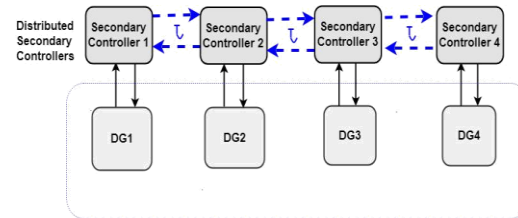


Fig. 26: Time delays in the distributed secondary control

DG_i gets information from DG_j through wired communication links like Ethernet, CAN, etc..., which induce network delay. Voltage of j^{th} DG deteriorate by network delay so direct axis voltage with network time delay is denoted by $V_{odj}(t - \tau)$. From this we can say that stability of the Microgrid is affected. neighborhood Global tracking error is affected. Rewrite Eqn. (22) with the effect of time delay,

$$e' = \sum_{j \in N_i} a_{ij}(V_{odi} - V_{odj}(t - \tau)) + g_i(V_{odi} - V_{ref}) \quad (50)$$

As a result, the transcendental term e^{-ts} will appear in the system characteristic equation, and stability of the DC Microgrid is inevitably affected.

A. Compensation of constant time delay

This section discusses about the time delay compensation in continuous time domain using Pade approximation technique. As shown in Fig. (26), due to the presence of networked medium between DG1, DG2, DG3 and DG4 all inputs available at the differential generators will suffer from communication

delay (τ) . V_{odj} is the signals available at the input of i^{th} DG's secondary controller and it is represented as:

$$V_{odj}(t) = V_{odj}(t - \tau)$$

where τ is communication delay.

Assumption 1: It is assumed that the communication delay is deterministic in nature satisfying,

$$\tau_l \leq \tau \leq \tau_u$$

Where τ_l and τ_u indicates lower and upper bound of communication delay.

As discussed earlier in order to handle communication delay, Pade approximation technique is introduced as follows:

$$L\{V_{odj}(t - \tau)\} = e^{-\tau s} L\{V_{odj}(t)\} \quad (51)$$

Applying first order approximation the above Eqn. (51) is written as,

$$L\{V_{odj}(t - \tau)\} \approx \frac{1 - \frac{\tau s}{2}}{1 + \frac{\tau s}{2}} L\{V_{odj}(t)\} \quad (52)$$

where $L\{V_{odj}(t)\}$ is Laplace transform of $V_{odj}(t)$. s is Laplace variable. Then, the variable V'_{odj} is defined as:

$$\frac{1 - \frac{\tau s}{2}}{1 + \frac{\tau s}{2}} L\{V_{odj}(t)\} = L\{V'_{odj}(t)\} + L\{V_{odj}(t)\}$$

where V'_{odj} is the variable to tackle the communication delay.

Applying inverse Laplace, we get

$$V_{odj} - \frac{\dot{V}_{odj}\tau}{2} = V'_{odj} + \frac{\dot{V}'_{odj}\tau}{2} - V_{odj} - \frac{\dot{V}_{odj}\tau}{2}$$

On further simplification we get,

$$\dot{V}'_{odj} = -\alpha V'_{odj} + 2\alpha V_{odj} \quad (53)$$

Where,

$$\alpha = \frac{2}{\tau}$$

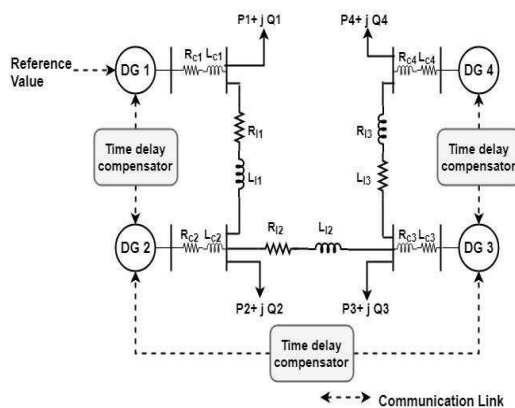


Fig. 27 Microgrid with delay compensation

Observing Eqn. (53), it is noticed that the communication delay at input of each DG's will be compensated through present variable V'_{odj} and parameter α that is computed through Pade approximation. By integrating Eqn.(53),

$$V'_{odj} = \int (-\alpha V'_{odj} + 2\alpha V_{odj}) dt \quad (54)$$

The change in V_{odj} reduces the adverse effect of time delay. In (63), after delay compensation $V_{odj}(t - \tau)$ is represented as V'_{odj} . By substituting the value of (54) in (53). We may get changes in global error,

$$e_{ci} = \sum_{j \in N_i} a_{ij} (V_{odi} - \int (-\alpha V'_{odj} + 2\alpha V_{odj}) dt) + g_i (V_{odi} - V_{ref}) \quad (55)$$

Where, e_{ci} is networked tracking error after compensation of time delay. Using this e_{ci} , rewrite the control law V_{ni} in (24),

$$V_{ni} = K_1 \text{sign}(e_{ci}) + K_2 \text{sign}(\dot{e}_{ci}) \quad (56)$$

$$V'_{ni} = K_1 \text{sign} \left[\sum_{j \in N_i} a_{ij} (V_{odi} - \int (-\alpha V'_{odj} + 2\alpha V_{odj}) dt) + g_i (V_{odi} - V_{ref}) \right] + K_2 \text{sign} \left[\sum_{j \in N_i} a_{ij} (\dot{V}_{odi} - (-\alpha V'_{odj} + 2\alpha V_{odj})) + g_i (\dot{V}_{odi}) \right] \quad (69)$$

The secondary control law reduces voltage variation occurs due to network time delay. Control law V'_{ni} sends to the power control of primary controller as shown in Fig. (20).

B. Simulation results

The proposed sliding mode control for secondary control method returns DG to their reference value. The sliding gains K_1 and K_2 are set to 8 and 5 respectively. In this case reference value for terminal voltage of DGs V_{ref} is set as 380V. It is assumed that Microgrid is islanded from the main grid. Initially all DGs controlled by primary controller. At $t=1$ sec, the distributed sliding mode secondary control is applied so all DGs are trying to reach its reference value. Normally Distance between two DGs are more so time delay occurs. Effect of time delay on voltage magnitude and all other parameter of all DGs are shown in two parts. Fig. (28) to (33) - (A) shows the effect of time delay compensated by Pade approximation method and Fig. (28) to (33) - (B) shows voltage magnitude, angular frequency, current, power and reactive power after using Pade approximation.

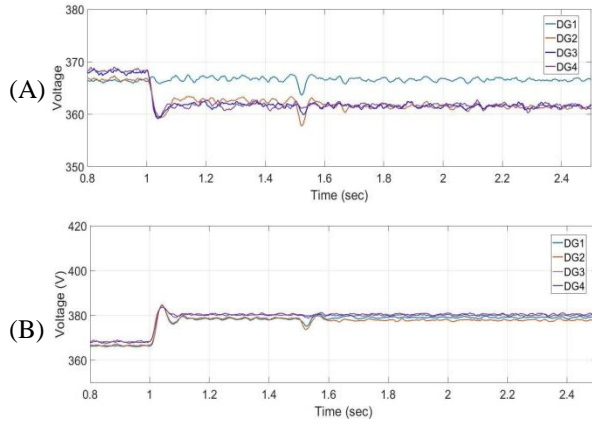


Fig. 28: Voltage waveform (A) Effect of time delay (B) After delay compensation.

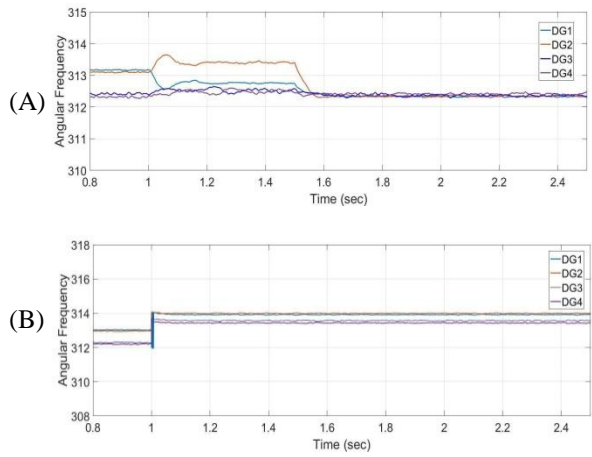


Fig. 29: Angular Frequency waveform (A) Effect of time delay (B) After delay compensation.

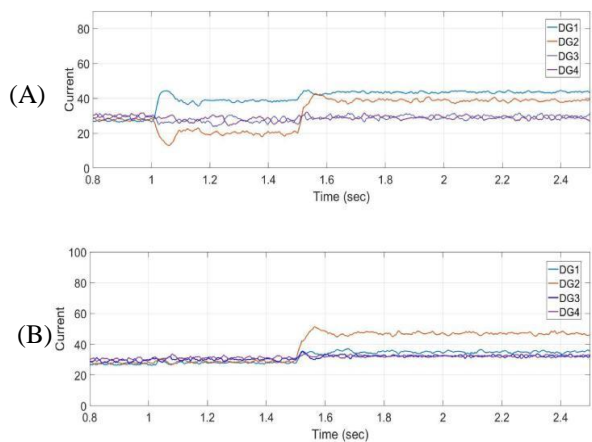


Fig. 30: Current waveform (A) Effect of time delay (B) After delay compensation.

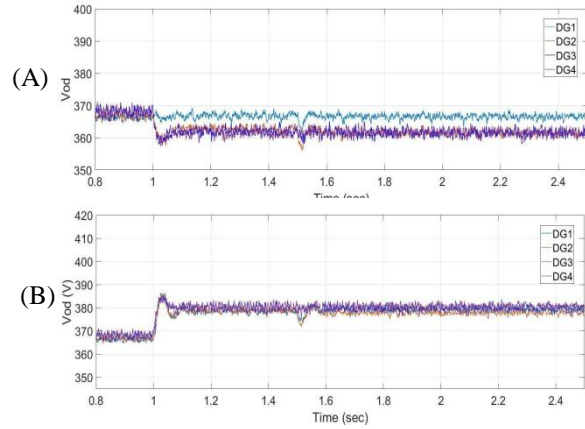


Fig. 31: Direct axis voltage waveform (A) Effect of time delay (B) After delay compensation.

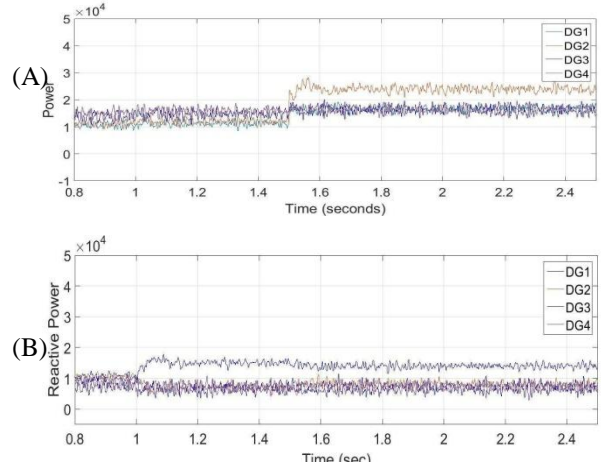


Fig. 32: Active Power waveform (A) Effect of time delay (B) After delay compensation.

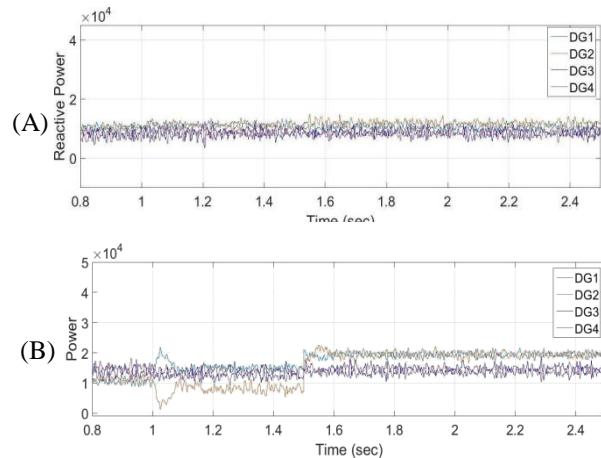


Fig. 33: Reactive Power waveform (A) Effect of time delay (B) After delay compensation.

8. Random Delay in Communication Network

In Microgrid recently random delay problem received much attention. The random delay generally depends on the characteristics of communication medium. In this section unique approach is presented for compensating the random delay.

A. Compensation of random delay

j^{th} DG is connected with i^{th} DG via communication link. j^{th} DG's voltage is denoted as V_{odj} . V_{odj} is the signal available at i^{th} DG's secondary controller and it is required as,

$$V_{odj}(t) = V_{odj}(t - \tau_r) \quad (57)$$

Where, τ_r is random uncertain delay.

From this we can say that stability of the Microgrid is affected. Neighborhood global tracking error is affected. Rewrite Eqn. (24) with the effect of time delay,

$$e'' = \sum_{j \in N_i} a_{ij}(V_{odi} - V_{odj}(t - \tau_r)) + g_i(V_{odi} - V_{ref}) \quad (58)$$

The random uncertain delay τ_r is modeled using exponential distribution with probability given by,

$$P_r\{\tau_r = d_v\} = E\{d_v\} = \beta_v; \quad V = 1, 2, \dots, q \quad (59)$$

Where,

β_v is positive scalar quantity

v is an event

$E\{d_v\}$ is an expectation of stochastic variable d_v .

d_v is rate of parameter.

The mathematical representation of v with exponential distribution is given as,

$$\beta_v = \lambda e^{-\lambda x} \quad (60)$$

d is rate parameter with $\lambda > 0$ and x is the random variable uniformly distributed over the interval $[0,1]$ and e equipotential term.

Thus using Pade approximation technique, Eqn. (57) is written as,

$$\mathcal{L}V_{odj}(t - \tau_r) \approx \frac{1 - \frac{\tau_r s}{2}}{1 + \frac{\tau_r s}{2}} \mathcal{L}V_{odj}(t) \quad (61)$$

Where $\mathcal{L}\{V_{odj}(t)\}$ is Laplace transform of $V_{odj}(t)$. s is Laplace variable. Then, the variable V'_{odj} is defined as:

$$\frac{1 - \frac{\tau_r s}{2}}{1 + \frac{\tau_r s}{2}} \mathcal{L}\{V_{odj}(t)\} = \mathcal{L}\{V'_{odj}(t)\} + \mathcal{L}\{V_{odj}(t)\}$$

Where, $V'_{odj}(t)$ is the variable to tackle the communication delay.

Applying inverse Laplace, we get

$$V_{odj} - \frac{\dot{V}_{odj}\tau_r}{2} = V'_{odj} + \frac{\dot{V}'_{odj}\tau_r}{2} - V_{odj} - \frac{\dot{V}_{odj}\tau_r}{2}$$

On further simplification, we get

$$\dot{V}'_{odj} = -\alpha V'_{odj} + 2\alpha V_{odj} \quad (62)$$

Where,

$$\alpha = \frac{2}{\tau}$$

Observing Eqn. (62), it is noticed that the communication delay at input of each DG's will be compensated through present variable V'_{odj} and parameter that is computed through Pad approximation. By integrating Eqn. (62),

$$V'_{odj} = \int (-\alpha V'_{odj} + 2\alpha V_{odj}) dt \quad (63)$$

The change in V_{odj} reduces the adverse effect of time delay. In (58), after delay compensation $V_{odj}(t - \tau)$ is represented as V'_{odj} . By substituting the Eqn. (63) in (57), we may get changes in global error,

$$e_{ri} = \sum_{j \in N_i} a_{ij}(V_{odi} - \int (-\alpha V'_{odj} + 2\alpha V_{odj}) dt) + g_i(V_{odi} - V_{ref}) \quad (64)$$

Where, e_{ri} is networked tracking error after compensation of random time delay. Using e_{ri} , rewriting the control law V_{ni} in (27),

$$V_{ni} = K_1 \text{sign}(e_{ri}) + K_2 \text{sign}(\dot{e}_{ri})$$

$$\begin{aligned} V''_{ni} = & K_1 \text{sign} \left[\sum_{j \in N_i} a_{ij}(V_{odi} \right. \\ & - \int (-\alpha V'_{odj} + 2\alpha V_{odj}) dt) \\ & + g_i(V_{odi} - V_{ref}) \left. \right] + K_2 \text{sign} \left[\sum_{j \in N_i} a_{ij}(\dot{V}_{odi} \right. \\ & - (-\alpha V'_{odj} + 2\alpha V_{odj})) + g_i(\dot{V}_{odi}) \left. \right] \end{aligned} \quad (65)$$

The secondary control law reduces voltage variation occurs due to network time delay. Control law V_{ni}^{00} sends to the power control of primary controller as shown in Fig. (22).

B. Simulation results

The proposed sliding mode control for secondary control method returns DG to their reference value. The sliding gains K_1 and K_2 are set to 8 and 5 respectively. In this case, reference value for terminal voltage of DGs V_{ref} is set as 380V. The random delay is set between 0 to 50 ms. The simulation results shown in

Figures (34) – (39) inferes improved performance compared to without compensation.

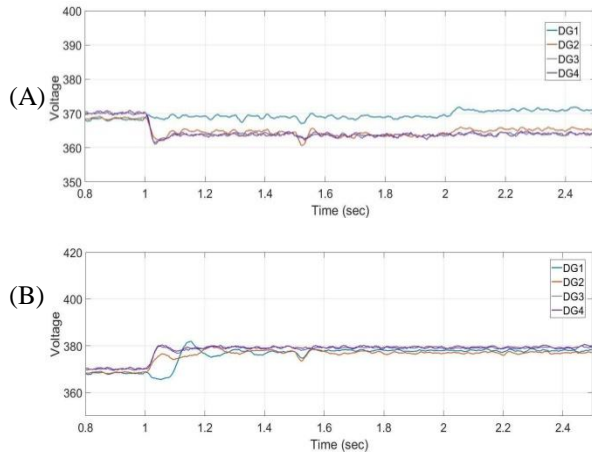


Fig. 34: Voltage waveform (A) Effect of random time delay (B) After delay compensation.

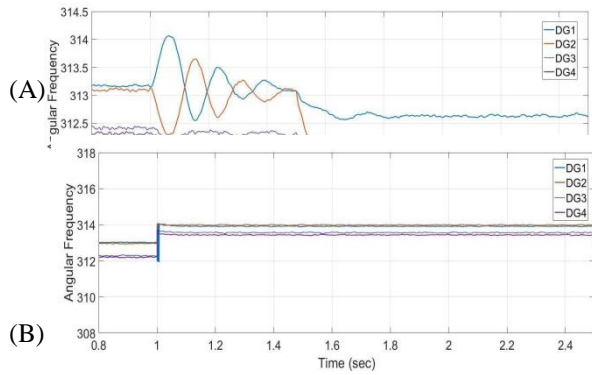


Fig. 35: Angular frequency waveform (A) Effect of random time delay (B) After delay compensation.

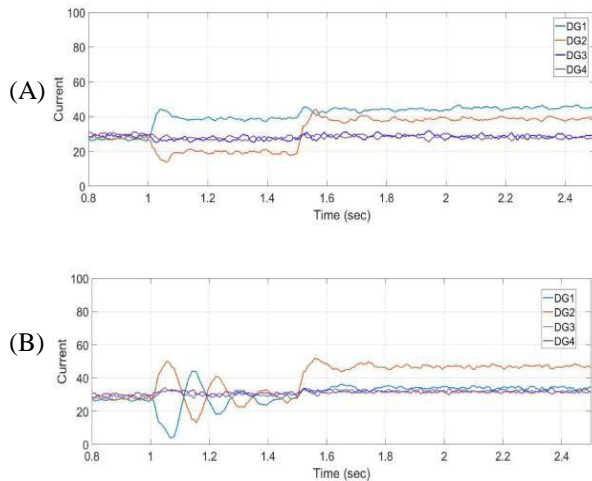


Fig. 36: Current waveform (A) Effect of random time delay (B) After delay compensation.

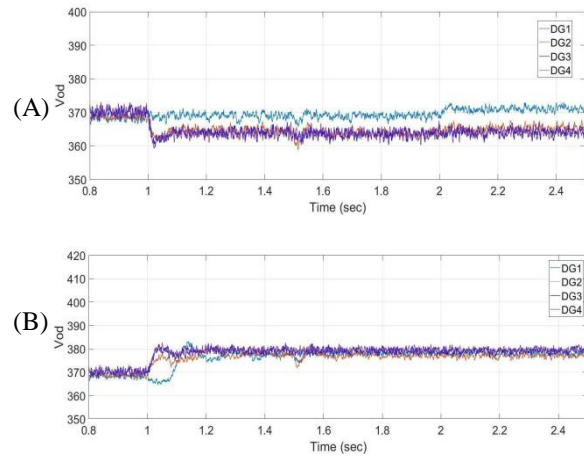


Fig. 37: Direct axis voltage waveform (A) Effect of random time delay (B) After delay compensation.

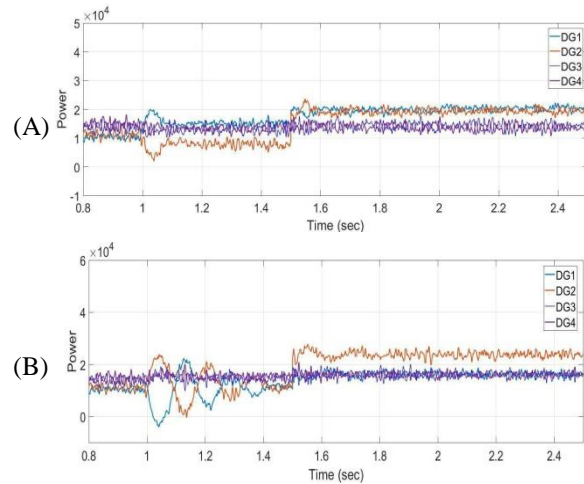


Fig. 38: Power waveform (A) Effect of random time delay (B) After delay compensation

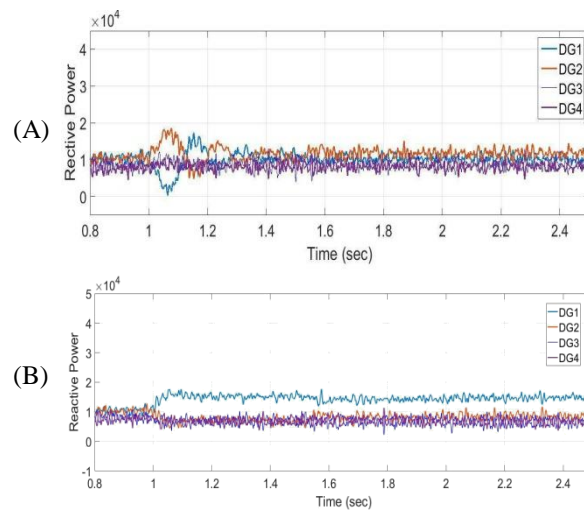


Fig. 39: Reactive power waveform (A) Effect of random time delay (B) After delay compensation.

9. Conclusion

In this paper, a distributed second order sliding mode controller with twisting algorithm is proposed for voltage and frequency restoration of an AC Microgrid. Both the delays namely the deterministic (constant) delay and random delay are compensated in the sliding surface. The deterministic delay is approximated by the padé approximation while random delay is compensated by exponential distribution method. The twisting algorithm of second order SMC is modified to design the distributed sliding mode control. The Secondary controller synchronize each DG and set its voltage and frequency to its reference value in finite time. The simulation results were carried out in two modes. without compensation and with compensation. It is inferred from simulation results that the performance of Microgrid is deteriorated due to time delay which is enhanced due to proposed algorithm under deterministic and random type delay.

REFERENCES

- [1] N. Pogaku, M. Prodanovic, and T. G. Green, "Modeling, analysis and testing of autonomous Microgrid of an inverter-based Microgrid," *IEEE Trans. Power Electron.*, vol. 22, no. 2, pp. 613-625, 2007.
- [2] A. Bidram and A. Davoudi, "Hierarchical structure of Microgrid control system," *IEEE Trans. Smart Grid*, vol. 3, no. 4, pp. 1963-1976, 2012.
- [3] A. Bidram, A. Davoudi, F. L. Lewis, and Z. Qu, "Secondary control of Microgrids based on distributed cooperative control of multi-agent systems," *IET Gener. Transm. Distrib.*, vol. 7, no. 8, pp. 822-831, 2013.
- [4] A. Bidram and F. L. Lewis, "Distributed Control Systems for Small-Scale Power Networks," *IEEE Control Syst. Mag.*, vol. 34, no. 6, pp. 56-77, 2014.
- [5] J. Lopes, C. Moreira, and A. Madureira, "Defining control strategies for Microgrids islanded operation," *IEEE Trans. Power Syst.*, vol. 21, no. 2, pp. 916-924, 2006.
- [6] Q. Shafiee, J. M. Guerrero, and J. C. Vasquez, "Distributed Secondary Control for Islanded Microgrids - A Novel Approach," *IEEE Trans. Power Electr.*, vol. 29, no. 2, pp. 1018-1031, 2014.
- [7] A. Pilloni, A. Pisano, and E. Usai, "Robust Finite Time Frequency and Voltage Restoration of Inverter-based Microgrids via Sliding Mode Cooperative Control," *IEEE Trans. Ind. Electron.*, vol. 65, no. 1, pp. 907-917, 2017.
- [8] Y. W. Li and C. N. Kao, "An accurate power control strategy for power-electronics-interfaced distributed generation units operating in a low-voltage multibus Microgrid," *IEEE Trans. Power Electron.*, vol. 24, no. 12, pp. 2977-2988, 2009.
- [9] J. M. Guerrero, J. C. Vasquez, J. Matas, L. G. De Vicuna, and M. Castilla, "Hierarchical control of droop-controlled AC and DC Micro-grids - A general approach toward standardization," *IEEE Trans. Ind. Electron.*, vol. 58, no. 1, pp. 158-172, 2011.
- [10] M. Reza Davoodi, Z. Gallehdari, I. Saboori, H. Rezaee, E. Semsar-kazerooni, N. Meskin, F. Abdollahi, and K. Khorasani, "An Overview of Cooperative and Consensus Control of Multiagent Systems." *Wiley Encyclopedia of Electrical and Electronics Engineering*, 2016.
- [11] M. Glavic, "Agents and Multi-Agent Systems : A Short Introduction for Power Engineers," pp. 1-21, 2006.
- [12] J. Qin, Q. Ma, Y. Shi, and L. Wang, "Recent advances in consensus of multi-agent systems: A brief survey," *IEEE Trans. Ind. Electron.*, vol. 64, no. 6, pp. 4972-4983, 2017.
- [13] Z. Li, Z. Duan, G. Chen, and L. Huang, "Consensus of Multi-agent Systems and Synchronization of Complex Networks: A Unified Viewpoint," *IEEE Trans. Circuits Syst. I Regul. Pap.*, vol. 57, no. 1, pp. 213-224, 2010.
- [14] M. C. Chandorkar, S. Member, and M. Deepakraj, "Control of Parallel Connected Inverters in Standalone ac Supply Systems," vol. 29, no. 1, pp. 136-143, 1993.
- [15] L. Meng, Q. Shafiee, G. F. Trecate, H. Karimi, D. Fulwani, X. Lu, and J. M. Guerrero, "Review on Control of DC Microgrids," *IEEE Journal of Emerging and Selected Topics in Power Electronics*, vol. 5, no. 3, pp. 928-948, 2017.
- [16] A. Bidram, A. Davoudi, F. L. Lewis, and S. S. Ge, "Distributed adaptive voltage control of inverter-based Microgrids," *IEEE Trans. Energy Convers.*, vol. 29, no. 4, pp. 862-872, 2014.
- [17] Y. Shtessel, "Sliding mode control and observation." New York: Springer, 2014.
- [18] A. Polyakov and A. Poznyak, "Lyapunov function design for finite-time convergence analysis: 'Twisting' controller for second-order sliding mode realization," *Automatica*, vol. 45, no. 2, pp. 444-448, 2009.

- [19] A. Levant, "Sliding order and sliding accuracy in sliding mode control," *International Journal of Control*, vol. 1247-1263, pp. 37-41, 2012.
- [20] O. Huber, V. Acary, B. Brogliato, and F. Plestan, "Discrete-time twisting controller without numerical chattering: Analysis and experimental results with an implicit method," *Proc. IEEE Conf. Decis. Control*, pp. 4373-4378, 2014.
- [21] A. Bidram, A. Davoudi, F. L. Lewis, and J. M. Guerrero, "Distributed Cooperative Secondary Control of Microgrids Using Feedback Linearization," *IEEE Trans. Power Syst.*, vol. 28, no. 3, pp. 3462-3470, 2013.
- [22] Q. Ali and S. Montenegro, "Role of graphs for multi-agent systems and generalization of Euler's Formula," *IEEE 8th International Conference on Intelligent Systems*, pp. 198-204, 2016.
- [23] F. Guo, C. Wen, J. Mao, and Y. D. Song, "Distributed Secondary Voltage and Frequency Restoration Control of Droop-Controlled Inverter-Based Microgrids," *IEEE Trans. Ind. Electron.*, vol. 62, no. 7, pp. 4355-4364, 2015.
- [24] J. Li and D. Zhang, "Backstepping and Sliding-Mode Techniques Applied to Distributed Secondary Control of Islanded Microgrids," *Asian Journal of Control*, vol. 20, no. 5, pp. 1-8, 2017.
- [25] M. Kosari and S. H. Hosseinian, "Decentralized Reactive Power Sharing and Frequency Restoration in Islanded Microgrid," *IEEE Trans. Power Syst.*, vol. 32, no. 4, pp. 2901-2912, 2017.
- [26] I. Serban, "Frequency restoration in Microgrids by means of distributed control with minimum communication requirements," *IEEE Int. Symp. Ind. Electron.*, pp. 2590-2595, 2014.
- [27] Z. Qu, J. W. J. Wang, and R. a. Hull, "Cooperative Control of Dynamical Systems With Application to Autonomous Vehicles," *IEEE Trans. Automat. Contr.*, vol. 53, no. 4, pp. 894-911, 2008.
- [28] J. Y. Hung, W. Gao, and J. C. Hung, "Variable structure control: a survey," *Ind. Electron. IEEE Trans.*, vol. 40, no. 1, pp. 2-22, 1993.
- [29] M. A. Setiawan, F. Shahnia, R. P. S. Chandrasena, and A. Ghosh, "Data communication network and its delay effect on the dynamic operation of distributed generation units in a Microgrid," *Asia-Pacific Power Energy Eng. Conf. APPEEC*, March, 2014.
- [30] D. Shah and A. Mehta, "Discrete-time sliding mode controller subject to real-time fractional delays and packet losses for networked control system," *Int. J. Control. Autom. Syst.*, vol. 15, no. 6, pp. 2690-2703, 2017.
- [31] D. Shah and A. Mehta, "Fractional delay compensated discrete-time SMC for networked control system," *Digit. Commun. Networks*, vol. 3, no. 2, pp. 112-117, 2017.
- [32] S. Liu, X. Wang, and P. X. Liu, "Impact of Communication Delays on Secondary Frequency Control in an Islanded Microgrid," *IEEE Trans. Ind. Electron.*, vol. 62, no. 4, pp. 2021-2031, 2015.
- [33] C. Macana, E. Mojica-Nava, and N. Quijano, "Time-delay effect on load frequency control for Microgrids," *IEEE Int. Conf. Networking, Sens. Control*, pp. 544-549, 2013.
- [34] M. Marwali and A. Keyhani, "Control of distributed generation systems - Part I: Voltages and currents control," *IEEE Trans. Power Electron.*, vol. 19, no. 6, pp. 1541-1550, 2004.
- [35] C. Ahumada, R. Cardenas, D. Saez, and J. M. Guerrero, "Secondary Control Strategies for Frequency Restoration in Islanded Microgrids With Consideration of Communication Delays," *IEEE Trans. Smart Grid*, vol. 7, no. 3, pp. 1430-1441, 2016.
- [36] J. Mongkoltanatas, D. Riu, and X. Lepivert, "H infinity controller design for primary frequency control of energy storage in islanding Microgrid," *15th Eur. Conf. Power Electron. Appl. EPE*, no. 1, 2013.
- [37] N. Dehkordi, N. Sadati, and M. Hamzeh, "Robust backstepping control of an interlink converter in a hybrid AC/DC Microgrid based on feedback linearisation method," *Int. J. Control*, vol. 90, no. 9, pp. 1990-2004, 2017.
- [38] Y. Wang, Z. Xia, Z. Jiang, and G. Xie, "A quasi-sliding mode variable structure control algorithm for discrete-time and time-delay systems," *IEEE proceeding Control Decis. Conf.*, pp. 107110, 2011.
- [39] Z. Gao, "Integral Sliding Mode Controller for an Uncertain Network Control System with Delay" *Computer Engineering and Networking*, 277, 31-38, 2013.
- [40] V. Utkin, "Variable structure systems with sliding modes," *IEEE Trans. Automat. Contr.*, vol. 22, no. 2, pp. 212-222, 1977.
- [41] H. Khalil, *Nonlinear Systems*. Prentice-Hall, New Jersey, USA, 1996.
- [42] K. D. Young, V. I. Utkin, and U. ozg"uner, "A control engineer's guide to sliding mode control," *IEEE Trans. Control Syst. Technol.*, vol. 7, no. 3, pp. 328-342, 1999.
- [43] M. Khan, Design and application of second order sliding mode control algorithms. Ph.D. thesis, The University of Leicester, Leicester, UK, 2003.
- [44] A. Levant, "Principles of 2-sliding mode design," *Automatica*, vol. 43, no. 4, pp. 576-586, 2007.

- [45] C. Zhang, W. Ma, and C. Sun, "A switchable high-speed fiber-optic ring net topology and its method of high-performance synchronization for large-capacity power electronics system," *Int. J. Electr. Power Energy Syst.*, vol. 57, pp. 335-349, 2014.
- [46] N. Langhammer and R. Kays, "Performance evaluation of wireless home automation networks in indoor scenarios," *IEEE Trans. Smart Grid*, vol. 3, no. 4, pp. 2252-2261, 2012.
- [47] A. G. Tsikalakis and N. D. Hatziargyriou, "Centralized control for optimizing Microgrids operation," *IEEE Trans. Energy Convers.*, vol. 23, no. 1, pp. 241-248, 2008.
- [48] K. T. Tan, S. Member, X. Y. Peng, S. Member, P. L. So, S. Member, Y. C. Chu, S. Member, and M. Z. Q. Chen, "Centralized Control for Parallel Operation of Distributed Generation Inverters in Microgrids," *IEEE Trans. Power Syst.*, vol. 3, no. 4, pp. 1977-1987, 2012.
- [49] K. Iniewski, *Smart grid infrastructure & networking*. 2013.
- [50] I. Serban and C. Marinescu, "Frequency Control Issues in Microgrids with Renewable Energy Sources," *Power*, no. L, pp. 1-6, 2011.